

Supplementary Information

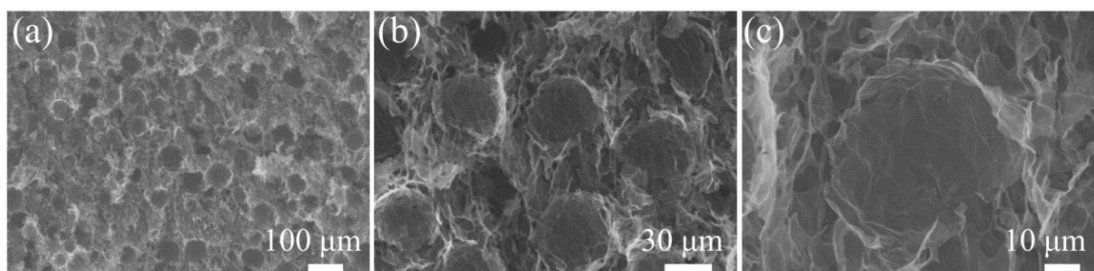


Fig. S1 (a–c) Scanning electron microscopy (SEM) images of 3D PS-free graphene foam prepared in oil-in-water system, showing the typically cellular networks.

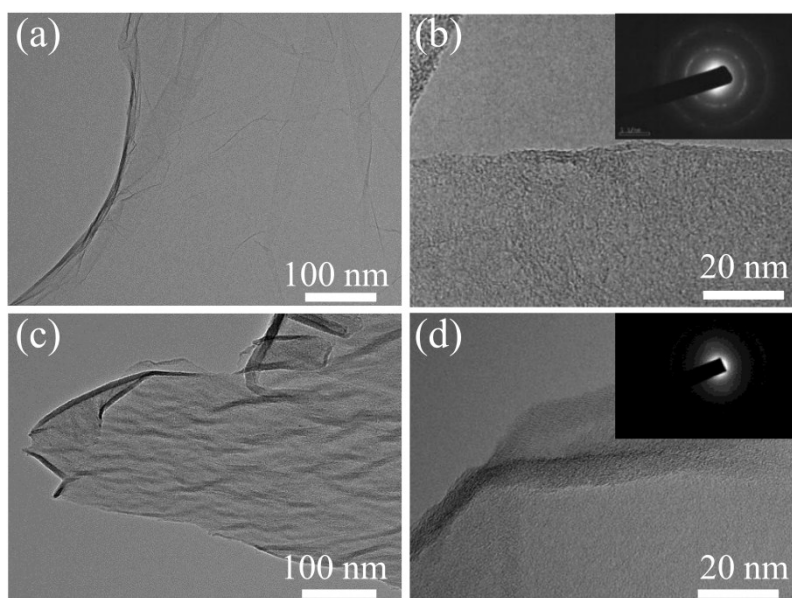


Fig. S2 (a, b) Transmission electron microscopy (TEM) images of original reduced graphene oxide (rGO) sheets at different magnifications. Inset of (b) is the corresponding electron diffraction patterns. (c, d) TEM images of PS₁₅/G-CF at different magnifications. Inset of (d) is the corresponding electron diffraction patterns. The electron diffraction spots of graphene sheets in (d) disappeared after combination with PS.

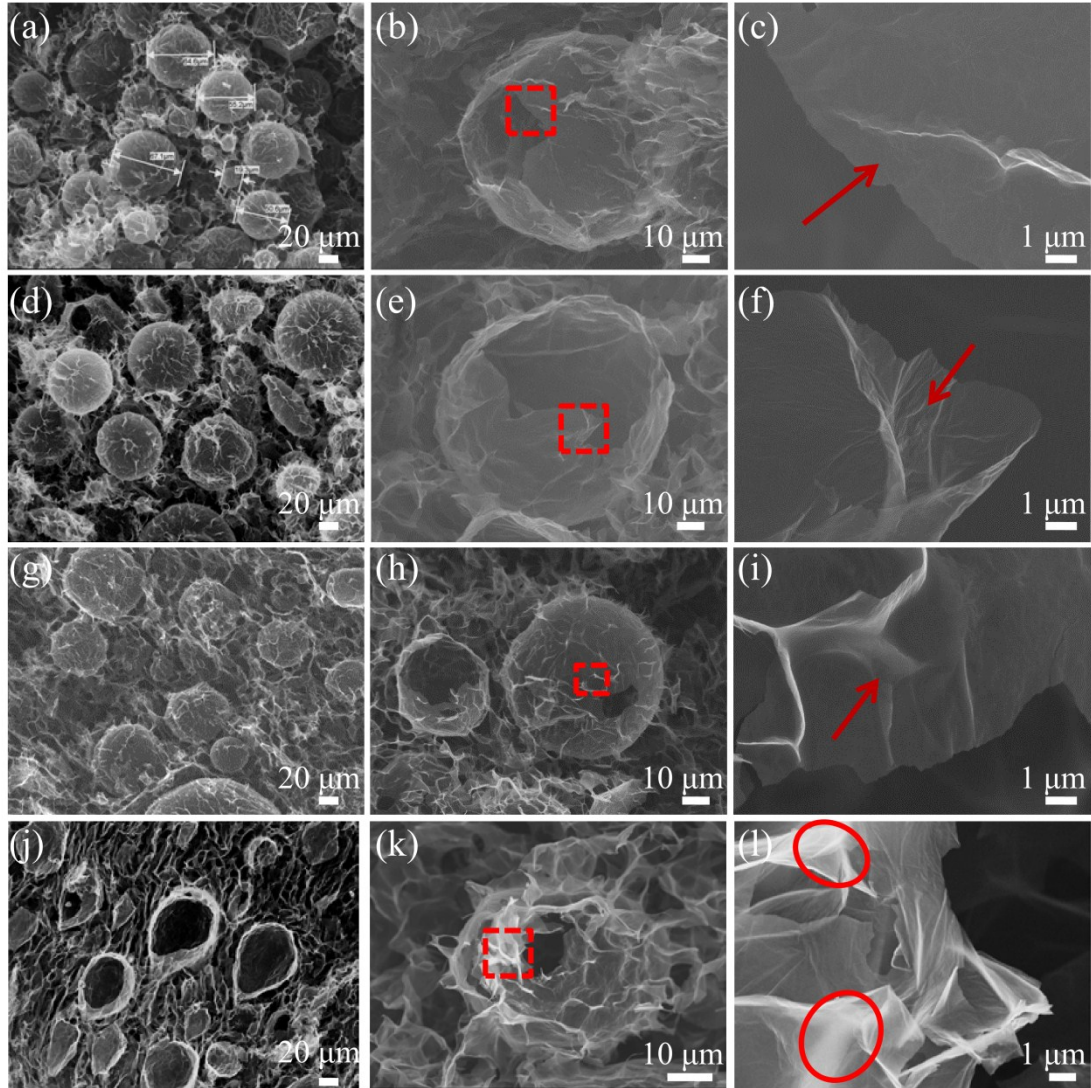


Fig. S3 (a, b) SEM images of PS₂₅/G-CF. (c) The corresponding enlarged image of square area in (b). (d, e) SEM images of PS₄₀/G-CF. (f) The corresponding enlarged image of square area in (e). (g, h) SEM images of PS₅₀/G-CF. (i) The corresponding enlarged image of square area in (h). (j, k) SEM images of PS₆₀/G-CF. (l) The corresponding enlarged image of square area in (k).

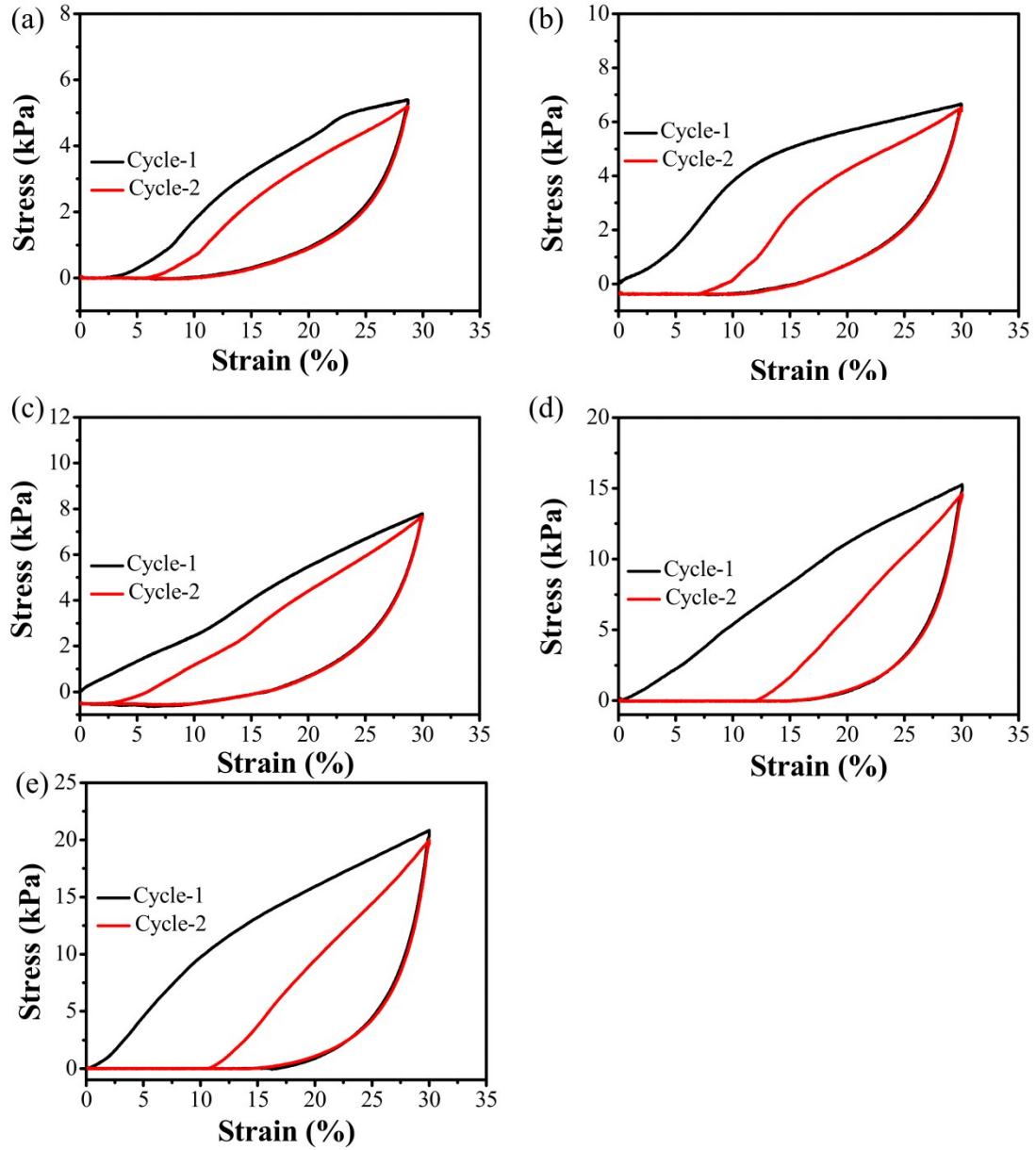


Fig. S4 The stress-strain curves of (a) PS₁₅/G-CF (b) PS₂₅/G-CF (c) PS₄₀/G-CF (d) PS₅₀/G-CF (e) PS₆₀/G-CF before thermal annealing. The PS_n/G-CFs shows no obvious elastic behaviors at low strain of 30%.

Table S1. The properties of PS_n/G-CFs with different weight percentage of PS.

Samples	Weight percentage of PS (wt%)	Density (mg cm ⁻³)	Maximum stain (%)	Max stress at max strain (kPa)	Conductivity (S m ⁻¹)
PS ₁₅ /G-CF	15	12.47	70	53.97	4.33
PS ₂₅ /G-CF	25	14.84	80	69.29	3.13
PS ₄₀ /G-CF	40	19.30	80	80.10	2.27
PS ₅₀ /G-CF	50	22.17	95	164.67	1.86
PS ₆₀ /G-CF	60	31.52	90	126	0.98

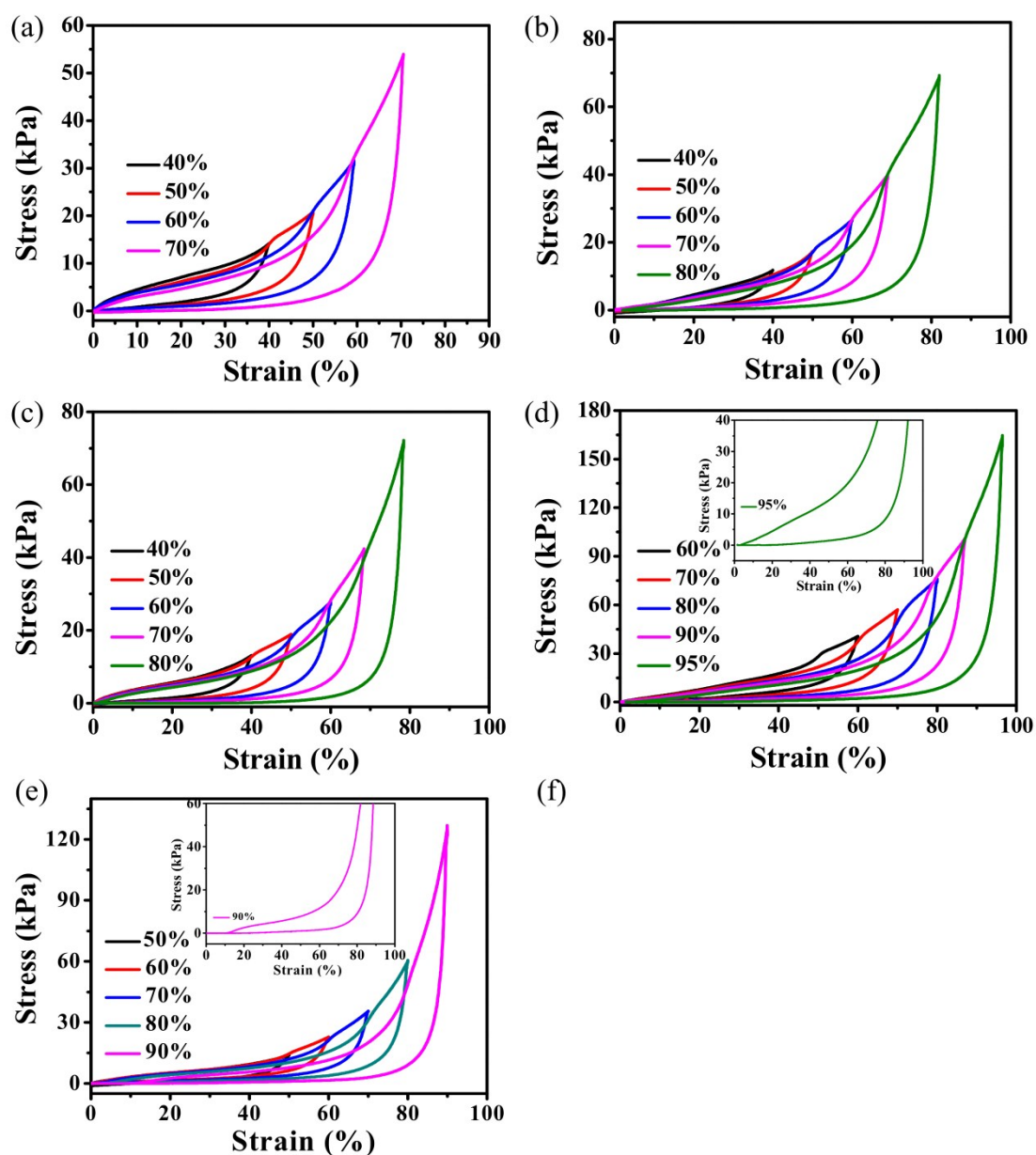


Fig. S5 The stress-strain curves of (a) PS₁₅/G-CF (b) PS₂₅/G-CF (c) PS₄₀/G-CF (d) PS₅₀/G-CF (e) PS₆₀/G-CF at different set strains. Inset in (d): The enlarged stress-strain curve of the sample at $\epsilon = 95\%$. Inset in (e): The enlarged stress-strain curve of the sample at $\epsilon = 90\%$.

Table S2. Mechanical properties of PS₅₀/G-CFs in this work compared with other previous reported carbon-based foams in recent years.

Samples	Density (mg cm ⁻³)	Maximum stain (%)	Max stress at max strain (kPa)	Ref.
This work	22.17	95	165	
Macroporous graphene monoliths	12.32	50	31.94	28
Graphene foam cellular networks	17	50	45	36
Poly(dimethylsiloxane)/graphene foam	–	90	43	38
Sponge-like carbonaceous aerogels	58	50	110	43
Commercial polyurethane/graphene foams	25-30	80	150	44
Commercial polyurethane sponge	25-30	80	12	45

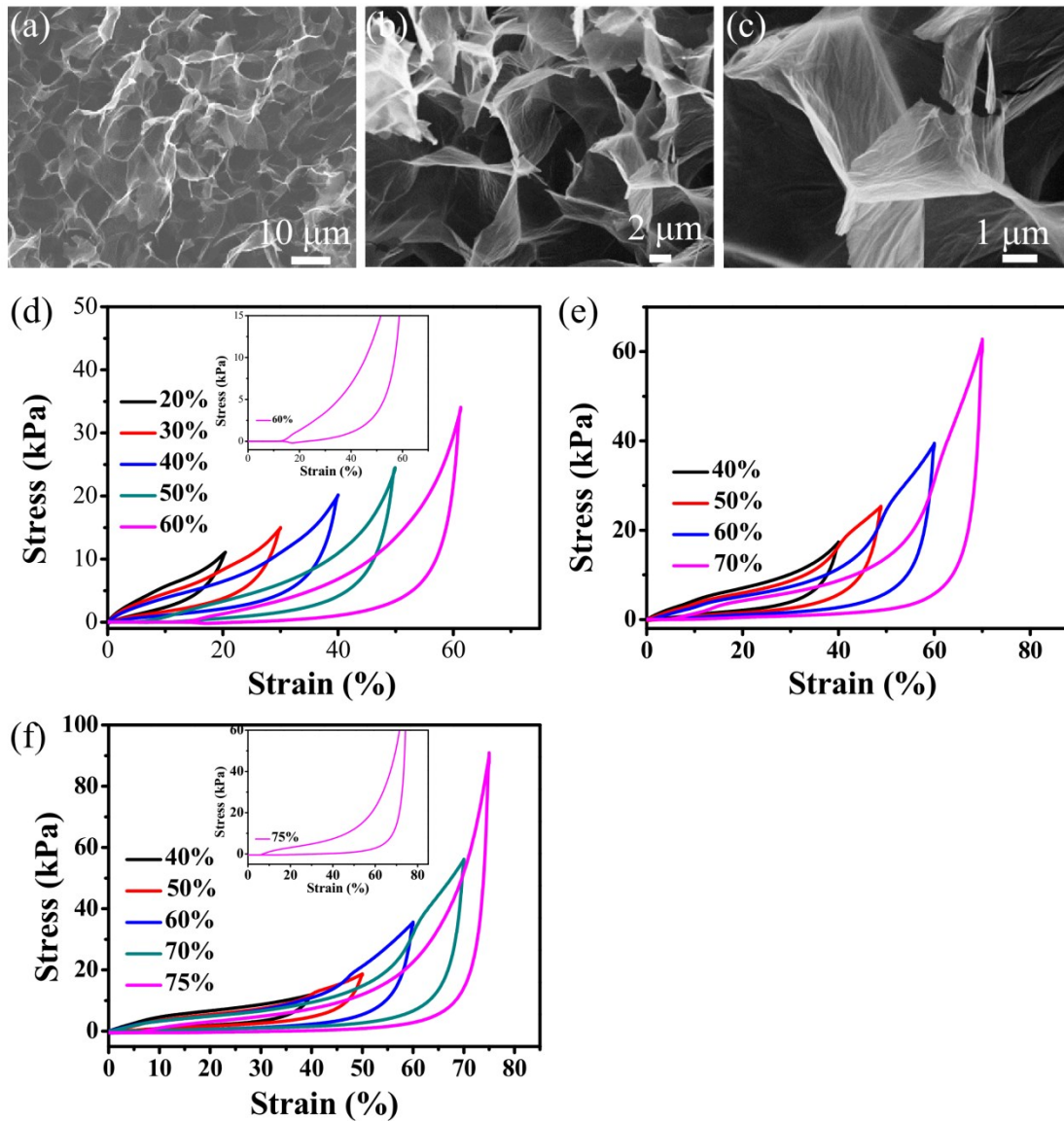


Fig. S6 SEM images of (a–c) 3D PS/G foam without capsule-like networks at different magnifications. The stress-strain curves of (d) PS-free 3D rGO foam with usual cellular networks prepared in oil-in-water system and (e) 3D PS₅₀/G foam without capsule-like structures. Inset: The enlarged stress-strain curve of the sample at $\epsilon = 60\%$. (f) The stress-strain curves of PS₅₀/G-CF with the thermal annealing temperature of 300 °C. Inset: The enlarged stress-strain curve of the sample at $\epsilon = 75\%$.

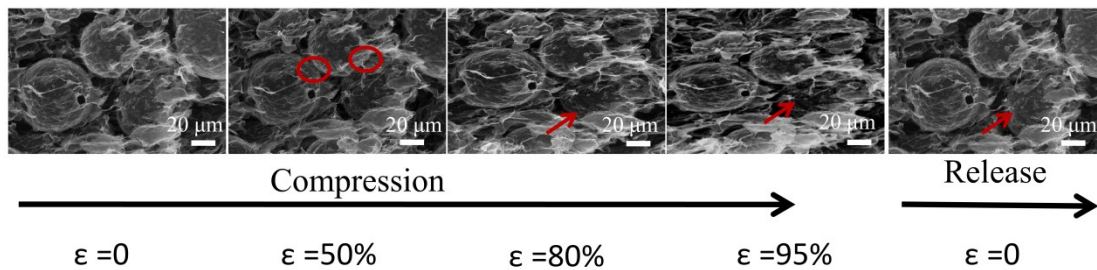


Fig. S7 SEM images of loading and unloading states of PS₅₀/G-CF during squeezing, the graphene capsules volume remained constant during the compression process.

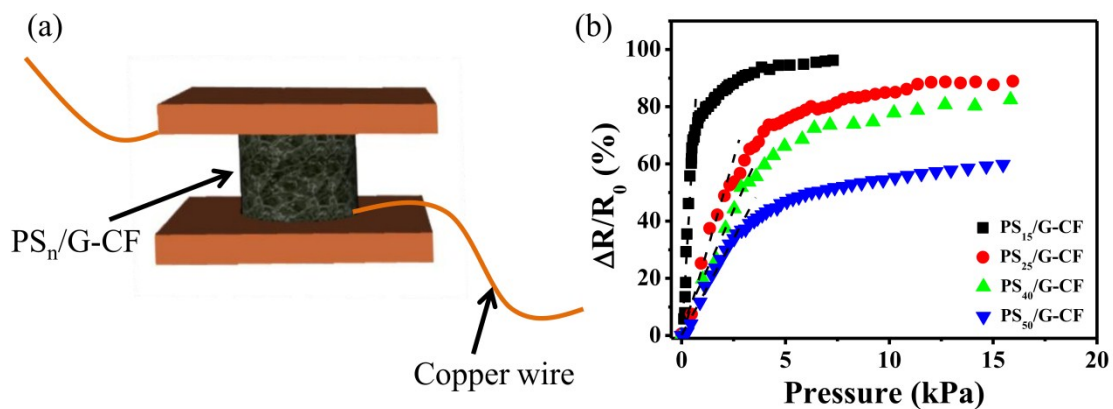


Fig. S8 (a) The illustration of the test setup for the dynamic resistance variation ratio. (b) Electrical responses of $PS_n/G-CFs$ ($n=15, 25, 40, 50$). The slope of each curve indicates the sensitivity of each sample to pressure.

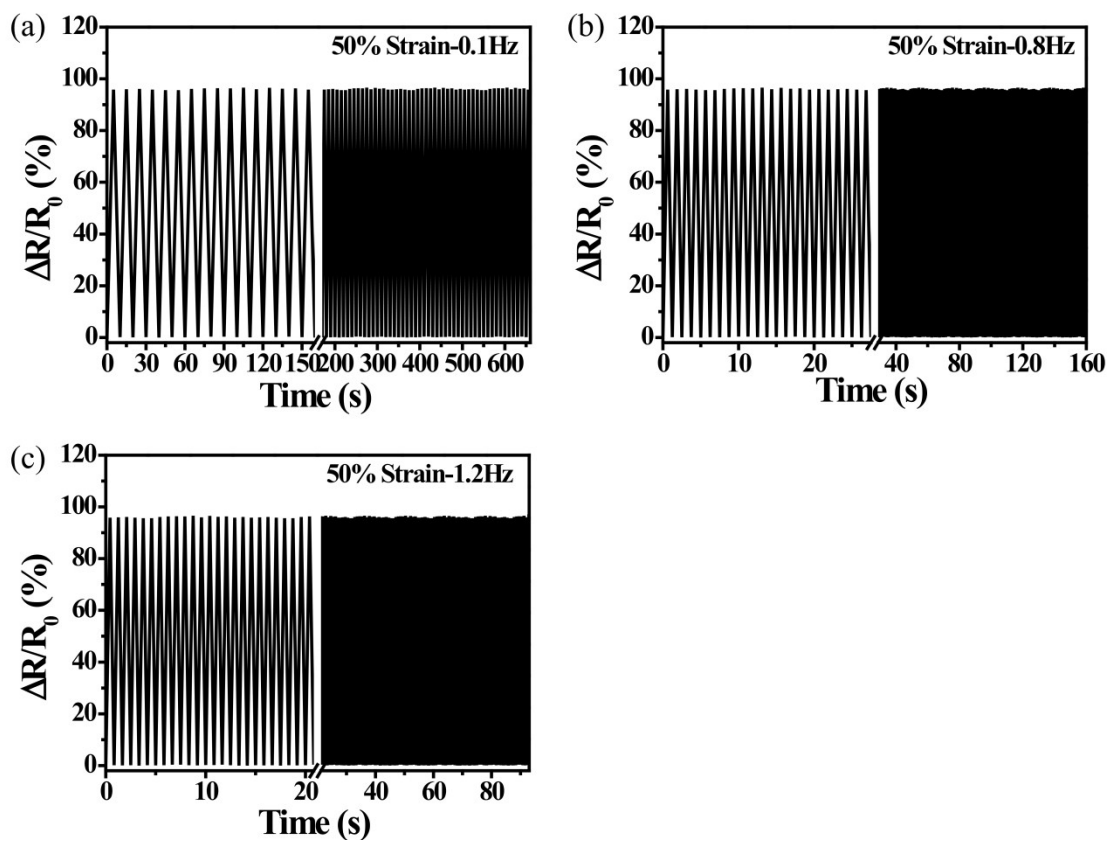


Fig. S9 Cycling stability test of $PS_{15}/G-CF$ under the applied strain of 50% with the loading frequency of (a) 0.1 Hz (b) 0.8 Hz and (c) 1.2 Hz, respectively.